Ultrashort soliton generation through higher-order soliton compression in a nonlinear optical loop mirror constructed from dispersion-decreasing fiber

P. K. A. Wai and Wen-hua Cao*

Photonics Research Center and Department of Electronic and Information Engineering, The Hong Kong Polytechnic University, Hung Hom, Hong Kong

Received June 27, 2002; revised manuscript received January 18, 2003

A novel technique to generate ultrashort fundamental solitons is proposed and demonstrated numerically. The technique utilizes both the multisoliton pulse-compression effect and the switching characteristics of a nonlinear optical loop mirror constructed from dispersion-decreasing fiber. We show that, in contrast to the conventional soliton-effect pulse compression in which compressed pulses are always accompanied by broad pedestals, the proposed technique can completely suppress pulse pedestals, and the compressed pulses propagate like fundamental solitons. Unlike the adiabatic-compression technique based on dispersion-decreasing fibers that are limited to input pulse widths <5 ps, the proposed technique does not require the adiabatic condition and therefore can be used to compress long pulses by use of reasonable fiber lengths. Furthermore, the scheme is more tolerant of initial frequency chirps than the adiabatic-compression technique, and it is shown that positive chirps are beneficial to ultrashort soliton generation. The influences of higher-order effects such as Raman self-scattering and third-order dispersion on soliton generation are also investigated, and it is found that Raman self-scattering can significantly enhance pulse compression under certain conditions.

OCIS codes: 060.4370, 190.5530, 320.5520, 320.5540, 060.1810.

1. INTRODUCTION

Soliton-based communication systems are leading candidates for ultra-high-speed long-haul lightwave transmission links because they offer the possibility of a dynamic balance between group-velocity dispersion (GVD) and self-phase modulation, the two effects that severely limit the performance of nonsoliton systems.[1] To date, soliton transmission experiments at 160 Gbits/s over 10 000 km have been successfully demonstrated.[2] One of the key elements of the system is a source of transform-limited pulses that are a few picoseconds wide. An attractive method for producing such short pulses is to make use of the nonlinear properties of the optical fiber itself in order to compress pulses generated from semiconductor lasers. Two widely adopted techniques are the soliton-effect[3–5] and adiabatic[6–10] pulse-compression techniques.

The mechanism of soliton-effect pulse compression is related to a fundamental property of the higher-order solitons in optical fibers. These solitons follow a periodic evolution pattern such that they go through an initial narrowing phase at the beginning of each period. With an appropriate choice of the fiber length, the pulse can be made to exit the fiber where it is narrowest. The drawback of the technique is that the quality of the compressed pulse is rather poor since a significant proportion of the pulse energy is contained in a broad pedestal rather than the compressed spike. For a pulse-compression factor of 60, up to 80% of the pulse energy is contained in the pedestal component.[5] These compressed pulses cannot be used as long-distance information carriers because the pedestals will lead to intersymbol interference.

Several techniques for pulse pedestal suppression have been implemented successfully. One of them is the intensity discrimination technique,[11,12] in which the fiber nonlinear birefringence induced by an intense pulse is used to modify the shape of the same pulse. As a result, the low-intensity tails of a pulse are blocked while the peak of the pulse is allowed to pass. Another technique[13–16] for pedestal suppression is to utilize a nonlinear optical loop mirror (NOLM). A NOLM can self-switch if a symmetry-breaking element such as an attenuator or an amplifier is placed in the loop. Counterpropagating pulses will therefore acquire different nonlinear phases. At recombination in the coupler, both reflected and transmitted outputs are produced. Since the transmission is intensity dependent, the loop length can be chosen such that the low-intensity pedestal is reflected while the higher-intensity pulse peak is transmitted, resulting in a pedestal-free transmitted pulse. However, the ability of both techniques to suppress the pedestal in the femtosecond region is severely limited by higher-order effects such as Raman self-scattering (RSS) and third-order dispersion (TOD) because, in general, the compressed pulses have to propagate through a relatively long fiber. Besides increasing the pulse width and reducing pulse energy, higher-order effects also severely degrade pulse quality in pedestal suppression of femtosecond pulses with a NOLM.[15] Simultaneous pulse compression and

0740-3224/2003/061346-10$15.00

pedestal suppression with NOLMs have also been demonstrated.[17–21] However, to our knowledge, no solitons were generated by this compression technique. References 17 and 18 showed the possibility of pulse compression by a NOLM containing an asymmetric coupler and a piece of uniform fiber[17] or a NOLM constructed from two different fibers with a symmetric coupler,[18] but the general optimization criteria for pulse compression were not studied. In Ref. 19, the transmitted pulses have strong frequency chirps. In order to realize pulse compression, an additional length of dispersion-compensated fiber must be spliced to the output end of the NOLM for chirp compensation. References 20 and 21 studied in detail higher-order soliton compression in an unbalanced NOLM constructed from a uniform fiber, where, although simultaneous pulse compression and pedestal suppression were achieved, the compressed pulse shapes deviate significantly from that of a soliton (see Fig. 3 of Ref. 20 and Fig. 2 of Ref. 21). The reason is that the loop length was optimized to achieve the maximum compression factor[20] or the maximum compression of the clockwise-propagating pulse.[21] These optimization criteria were not appropriate to produce compressed solitonlike pulses.

Pulse compression with minimal or no pedestal component can be achieved by the adiabatic technique. Compressed fundamental solitons have been obtained experimentally by use of dispersion-decreasing fibers[6–10] (DDFs), steplike[22] or comblike[23] dispersion-profiled fibers, and constant-dispersion fibers with distributed amplification.[24] The compression mechanism is based on the fact that a small variation, such as second-order dispersion or amplification, perturbs the equilibrium between dispersion and nonlinearity of a soliton in such a way that, when, for example, the dispersion decreases, the soliton is compressed. The main advantages of this technique is the ability to generate femtosecond solitons with input power significantly lower than that for soliton-effect pulse compression. The main drawback is that very long lengths of fiber are required when the input pulse width exceeds several picoseconds. It was shown[8] that, for a 10-ps input pulse, the required fiber length increases to 20 km. With such long fibers, loss will significantly reduce the effective amplification provided by the decreasing dispersion. Although several methods[8,25–27] have been used to overcome this difficulty, the decreases in fiber length were not significant.

In this paper, we demonstrate that ultrashort solitonlike pulses can be generated through higher-order soliton compression in a NOLM constructed from a dispersion-decreasing fiber (DDF) (hereafter, we call it DD-NOLM). Unlike the adiabatic-compression technique that is limited to input pulse widths <5 ps, the proposed scheme does not require the adiabatic condition and therefore can be used to compress a longer pulse with reasonable fiber lengths. Furthermore, the proposed scheme is more tolerant of initial frequency chirps and higher-order effects than the adiabatic-compression technique. This scheme is distinct from that of Refs. 20 and 21 not only in the NOLM structure but also in the optimization criteria for pulse compression. We note that previous work on a DD-NOLM focused on the switching characteristics of the device.[28,29] A DD-NOLM was also used as an intensity-dependent transmission element in a passively mode-locked fiber laser,[30] but the mode locking was based on adiabatic pulse compression in the loop in which the loop length increases exponentially with input pulse width.

2. ADIABATIC COMPRESSION OF FUNDAMENTAL SOLITONS IN DISPERSION-DECREASING FIBER

Before we investigate pulse compression in a DD-NOLM, it is useful to discuss the adiabatic compression technique based on DDF. This technique differs from the soliton-effect compression in that fundamental solitons rather than higher-order solitons are launched into the fiber. Pulse compression is achieved by manipulating the stability of these pulses to weak perturbations such as gain or dispersion. In the case of a fundamental soliton propagating along a DDF, the dispersion is monotonically and smoothly decreased from an initial value to a smaller value at the fiber end. If the dispersion variation is sufficiently gradual, the input soliton will be compressed adiabatically. Including fiber loss and higher-order effects, compression of fundamental solitons in a DDF can be described by a modified nonlinear Schrödinger equation, which, in normalized coordinates, takes the form[31]

$$i\frac{\partial u}{\partial \xi} + \frac{1}{2}p(\xi)\frac{\partial^2 u}{\partial \tau^2} + |u|^2 u + i\Gamma u = i\delta\frac{\partial^3 u}{\partial \tau^3} - is\frac{\partial}{\partial \tau}(|u|^2 u) + \tau_R u\frac{\partial |u|^2}{\partial \tau}, \quad (1)$$

where $u(\xi, \tau)$ is the normalized pulse envelope in soliton units and

$$\xi = \frac{z|\beta_2(0)|}{T_0^2}, \qquad \tau = \frac{t - z/v_g}{T_0}, \qquad p(\xi) = \left|\frac{\beta_2(\xi)}{\beta_2(0)}\right|, \quad (2)$$

$$\delta = \frac{\beta_3}{6|\beta_2(0)|T_0}, \qquad s = \frac{2}{\omega_0 T_0},$$

$$\tau_R = \frac{T_R}{T_0}, \qquad \Gamma = \frac{\alpha}{2}\frac{T_0^2}{|\beta_2(0)|}. \quad (3)$$

In Eqs. (2) and (3), $\beta_2(0)$ is the initial GVD coefficient of the DDF, β_3 is the TOD coefficient that is assumed to be constant along the DDF, v_g is the group velocity, ω_0 is the carrier frequency, T_0 is the half-width (at the $1/e$-intensity point) of the input pulse, T_R is the Raman resonant time constant (typically 3 fs for ordinary silica fibers), $p(\xi)$ governs the GVD variation along the DDF, and α is the attenuation constant. The parameters δ, s, and τ_R account for the effects of TOD, self-steepening, and RSS, respectively.

For a DDF of normalized length ξ_L, the ratio of input to output GVD coefficients,

$$G_{\text{eff}} = \beta_2(0)/\beta_2(\xi_L), \quad (4)$$

is commonly called the effective amplification of the fiber. Very high effective amplifications ($\beta_2(\xi_L) \approx 0$) cannot be

realized in practice because of the inherent small dispersion fluctuations associated with the manufacturing process, the wavelength dependence of the GVD coefficient, and the small fluctuations in the wavelength of the laser source. The maximum effective amplification was ~20 for soliton compression in DDFs.[7,8,32]

If the input to the DDF is a fundamental soliton of the form

$$u(0, \tau) = A \operatorname{sech}(A\tau), \tag{5}$$

and the dispersion variation along the DDF is sufficiently gradual, it has been shown[32,33] that the soliton will be compressed to

$$u(\xi_L, \tau) = \sqrt{G_{\text{eff}}} A \exp(-2\Gamma\xi_L)\operatorname{sech}[G_{\text{eff}} A \exp(-2\Gamma\xi_L)\tau] \times \exp\left\{ i \frac{A^2}{8\Gamma}[1 - \exp(-4\Gamma\xi_L)] \right\}, \tag{6}$$

in the absence of higher-order effects after a normalized length ξ_L.

In the ideal case ($\Gamma = 0$), Eq. (6) reduces to

$$u(\xi_L, \tau) = \sqrt{G_{\text{eff}}} A \operatorname{sech}(G_{\text{eff}} A\tau)\exp(iA^2\xi_L/2). \tag{7}$$

We define the compression factor, F_c, as the ratio of the full width at half-maximum (FWHM) of the input soliton to that of the compressed soliton. Then from Eqs. (5) and (7), the compression factor in the ideal case is equal to G_{eff}, and the soliton intensity is amplified by a factor of G_{eff}.

For a hyperbolic-secant pulse with peak power P_{peak} and pulse width T_{FWHM}, its energy is given by

$$E = 2P_{\text{peak}} \frac{T_{\text{FWHM}}}{1.763}. \tag{8}$$

Adiabatic compression means that all the energy of the pulse remains localized in the compressed pulse. From Eqs. (5) and (7), the compression is adiabatic, since the energy contained in the compressed soliton is equal to that of the input soliton.

Fiber loss leads to pulse broadening. From Eq. (6), the final compression factor is now given by

$$F_c = G_{\text{eff}} \exp(-2\Gamma\xi_L), \tag{9}$$

i.e., F_c is reduced by a factor of $\exp(2\Gamma\xi)$. For example, we consider the compression of a soliton with initial width of $T_{\text{FWHM}} = 10$ ps ($T_0 = 5.67$ ps). The DDF is assumed to have an initial GVD coefficient of $\beta_2(0) = -20\ \text{ps}^2/\text{km}$ and an effective amplification of $G_{\text{eff}} = 20$. Fiber loss is given by $\alpha = 0.046\ \text{km}^{-1}$ ($\Gamma = 0.037$). A typical normalized DDF length of $\xi_L = 10$ should be used to ensure a gradual dispersion variation along the DDF such that the compressed pulse has a high quality.[8,32] Thus from Eqs. (2) and (9), the DDF length is 16 km and the compression factor is reduced by a factor of 2. Note that both the fiber length and the loss parameter Γ increase exponentially with input soliton width. For $T_{\text{FWHM}} > 20$ ps, the DDF length is longer than 64 km, and the soliton ceases to compress.

3. HIGHER-ORDER SOLITON COMPRESSION IN DD-NOLM

In Section 2, it was shown that high-quality compression of fundamental solitons can be achieved with the adiabatic-compression technique. However, the required fiber length increases exponentially with the initial soliton width, and the compression factor is decreased by fiber loss. Thus the adiabatic-compression technique is generally not suitable for compression of pulses longer than 5 ps. On the other hand, higher-order soliton compression in a fiber line can achieve large compression factors with very short fibers, but the pulse quality is poor. In this section, we show that the difficulty can be overcome through higher-order soliton compression in a DD-NOLM. We also show that this scheme is more tolerant of initial frequency chirps and higher-order effects than previous compression techniques.

A. Demonstration of the Technique

Figure 1 shows the configuration of the DD-NOLM, which consists of a 50/50 coupler and a DDF with the dispersion coefficient decreasing in the clockwise direction. The input pulse u_1 is launched into port 1, and the compressed pulse u_2 is obtained at port 2. In normalized coordinates defined in Eqs. (1)–(3), the input pulse is assumed to be a higher-order soliton of the form

$$u_1(0, \tau) = N \operatorname{sech}(\tau), \tag{10}$$

where N is the soliton order and is related to the physical parameters by

$$N^2 = \frac{\gamma P_0 T_0^2}{|\beta_2(0)|}, \tag{11}$$

where γ is the nonlinearity coefficient (assumed to be a constant) of the DDF and P_0 is the peak power of the input pulse. The input pulse is split at the coupler according to[34]

$$u_3(0, \tau) = \sqrt{\alpha} u_1(0, \tau) = N\sqrt{\alpha} \operatorname{sech}(\tau), \tag{12}$$

$$u_4(0, \tau) = i\sqrt{1 - \alpha} u_1(0, \tau) = iN\sqrt{1 - \alpha} \operatorname{sech}(\tau), \tag{13}$$

where u_3 and u_4 are the field amplitudes right after the coupler and α:(1−α) is the power-coupling ratio. We have chosen $\alpha = 0.5$ throughout this paper. If the incident pulse duration is much shorter than the time to transverse the loop length and the pulse duration is also much shorter than $1/R$, where R is the pulse repetition rate, the interaction between counterpropagating fields

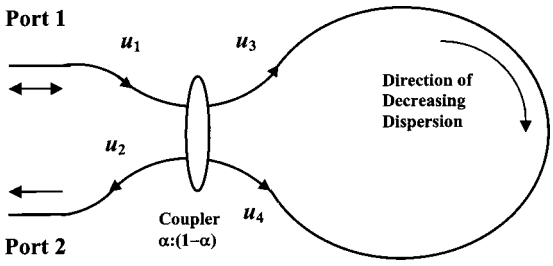

Fig. 1. Schematic of the DD-NOLM. Input pulses are launched into port 1, and compressed pulses are obtained from port 2.

can be neglected. The pulse evolution can then be described by Eq. (1). Note that the two pulses experience different dispersion profiles in the loop, i.e., the clockwise pulse initially experiences a dispersion G_{eff} times larger than the counterclockwise pulse does. In the following, Eq. (1) is solved numerically with the split-step Fourier method. After traveling around the loop, the counterpropagating pulses recombine at the coupler. The compressed pulse u_2 can be calculated with the coupler equations described in Ref. 34.

For illustration, we consider the compression of a sixth-order soliton [i.e., $N = 6$ in Eq. (10)] with an initial width $T_{\text{FWHM}} = 30$ ps ($T_0 \approx 17$ ps). The DDF has a linear dispersion profile with an effective amplification $G_{\text{eff}} = 3$. Using typical values of $\beta_2(0) = -20\,\text{ps}^2/\text{km}$ and $\gamma = 5\ \text{W}^{-1}\text{km}^{-1}$ for silica fibers near 1.55 μm, we find that the incident pulse has a peak power of 0.5 W. Fiber loss is included with $\alpha = 0.046\ \text{km}^{-1}$ ($\Gamma \approx 0.332$). We first neglected higher-order effects, which is a reasonable assumption for an input pulse width longer than 10 ps. The solid curves in Figs. 2(a) and 2(b) show the temporal shapes of the compressed (transmitted) pulse in linear and logarithmic scale, respectively, which is obtained by choosing the loop length, while G_{eff} has a fixed value of 3, to minimize the pedestal of the compressed pulse. The optimum loop length is 4.86 km ($\xi = 0.336$), and the compression factor is 4.76. The dashed curves in Figs. 2(a) and 2(b) represent a hyperbolic-secant pulse having the same peak intensity and FWHM pulse width as those of the compressed pulse. Figure 2(c) shows the spectrum, and Fig. 2(d) shows the frequency chirp (solid curve) and the shape (dashed curve) of the compressed pulse. The intensities of the pulse shape and spectrum are normalized with respect to the incident pulse, respectively. Figures 2(a) and 2(b) show that the compressed pulse is very close to a hyperbolic-secant pulse. From its peak intensity and width, the pulse is estimated to be

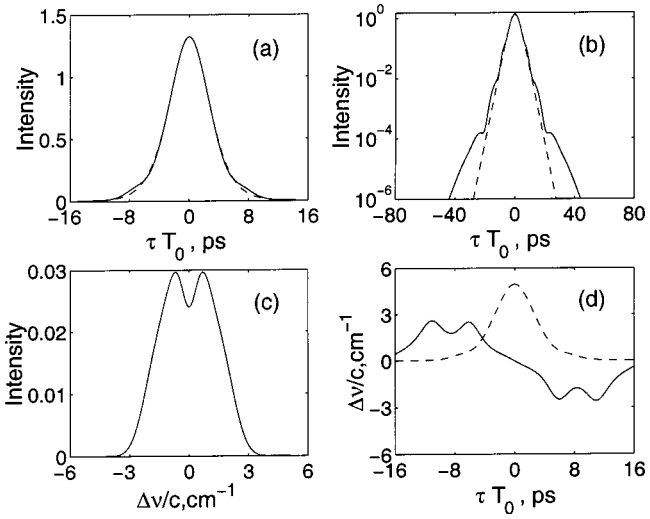

Fig. 2. Temporal shapes of the transmitted pulse in (a) linear and (b) logarithmic scale. (c) Spectrum and (d) frequency chirp (solid curve) and pulse shape (dashed curve) of the transmitted pulse. The dashed curves in (a) and (b) represent a hyperbolic-secant pulse having the same peak intensity and width (FWHM) as those of the transmitted pulse. The parameters are $N = 6$, $T_{\text{FWHM}} = 30$ ps, $G_{\text{eff}} = 3$, $\Gamma = 0.332$, and $\xi = 0.336$.

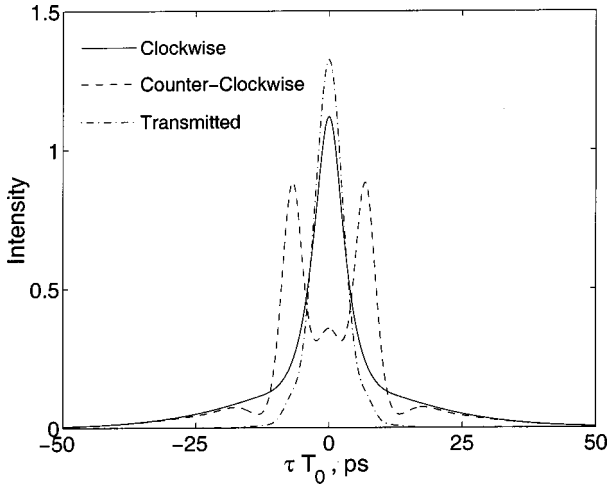

Fig. 3. Clockwise (solid curve) and counterclockwise (dashed curve) traveling pulses before recombination. The dash-dotted curve shows the transmitted pulse.

close to a fundamental soliton with a soliton order of 1.45. The pedestal of the compressed pulse is very small. We define the pedestal energy as the relative difference between the total energy, E_{TOTAL}, of the compressed pulse and the energy of the hyperbolic-secant pulse shown by the dashed line of Fig. 2(a), i.e.,

$$\text{pedestal energy } (\%) = \frac{|E_{\text{total}} - E_{\text{sech}}|}{E_{\text{total}}} \times 100\%. \tag{14}$$

Note that the energy of a hyperbolic-secant pulse with peak power P_{peak} and pulse width T_{FWHM} is given by Eq. (8). Using Eq. (14), the pedestal energy of the compressed pulse is only 1.3%.

Figure 2(c) shows that the spectrum of the compressed pulse is also close to a hyperbolic-secant shape except for a small notch in the central region, probably originating from the frequency chirps around the pulse pedestal. We note that the chirp across the main pulse is very small. The time–bandwidth product is 0.37, which is close to transform-limited value 0.315 of a hyperbolic-secant pulse. Figure 3 shows the clockwise (solid curve) and counter-clockwise (dashed curve) pulses after they travel around the loop but before recombination at the coupler under conditions identical to those of Fig. 2. The transmitted pulse is also shown by the dash-dotted curve. We observed that, although the shapes of both the clockwise and counter-clockwise pulses deviate significantly from a hyperbolic-secant, the transmitted pulse has a hyperbolic-secant shape.

The soliton pulse generation results from both of the soliton-effect compression of the counterpropagating pulses and the switching characteristics of the DD-NOLM. Since the loop is asymmetric, the compression of the counterpropagating pulses are different, and the two pulses acquire different phase shifts when they recombine at the coupler. At the optimum loop length, the switching condition is satisfied for the central peak but not for the rest of the pulse, leading to a pedestal-free compressed pulse. The optimum loop length is chosen such that the compressed pulse approaches a hyperbolic-secant

pulse, i.e., the pedestal of the compressed pulse is the smallest. This optimization criterion is different from that of Refs. 20 and 21, where the loop length was chosen such that the transmitted pulse[20] or the clockwise propagating pulse[21] is compressed optimally. Figure 4 shows the local compression factors of the counterpropagating pulses during their evolution in the loop under the same condition as that of Fig. 2. The optimum loop length for soliton generation is longer than that for the counterpropagating pulses to achieve maximum compression.

To study the stability of the compressed pulse, we couple the compressed pulse of Fig. 2 into a constant-dispersion lossless fiber with a dispersion coefficient identical to the initial dispersion coefficient $\beta_2(0)$ of the DDF loop. Figure 5 shows the evolution over a fiber length of 22.7 km, which corresponds to 23 soliton periods in terms of the initial pulse width (6.3 ps). The pulse broadens initially because of the negative chirp [shown in Fig. 2(d)]. It then compresses, since its intensity is higher than that of a fundamental soliton. As the propagation continues, the pulse approaches a fundamental soliton that is narrower than the incident pulse. The variation of the pulse width is due to the initial frequency chirp. We have tried to suppress the pulse-width fluctuation by varying the incident pulse power (which can be done by placing a tunable attenuator at the input end of the constant-dispersion fiber), but the result is not satisfactory. The general feature of pulse evolution is the same except that the output pulse width increases when the input pulse power decreases.

B. Effects of Loop Characteristics and Initial Soliton Order

The above results demonstrated the compression of a sixth-order soliton in a DD-NOLM for a particular loop length and a fixed effective amplification (G_{eff}). In this subsection, the effects of loop length, effective amplification, and incident soliton order are studied. Figure 6 shows the compression factor and corresponding pedestal energy as a function of the loop length. The input soliton in all cases is the same as that used for Fig. 2 (i.e., $N = 6$, $T_{\text{FWHM}} = 30$ ps). The DDF in each case has a same dispersion-decreasing rate as before, except that the length of the DDF is varied. Figure 6 shows that high-quality pulses with pedestal energy less than 2% can be achieved over a relatively wide range of the loop length (4.6–4.9 km).

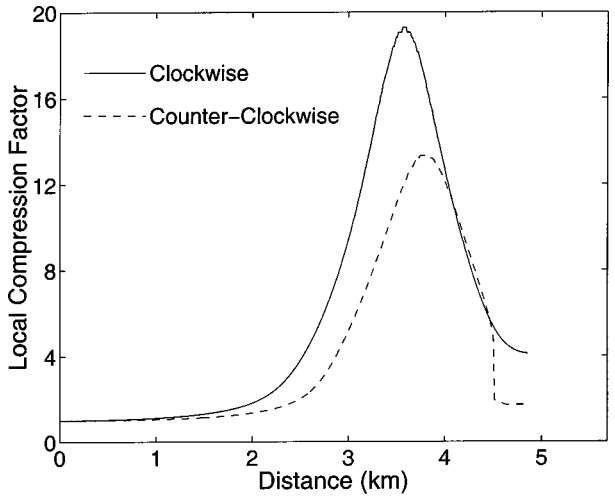

Fig. 4. Local compression factors of the clockwise (solid curve) and counterclockwise (dashed curve) pulses during their evolution in the loop under the same conditions as those of Fig. 2.

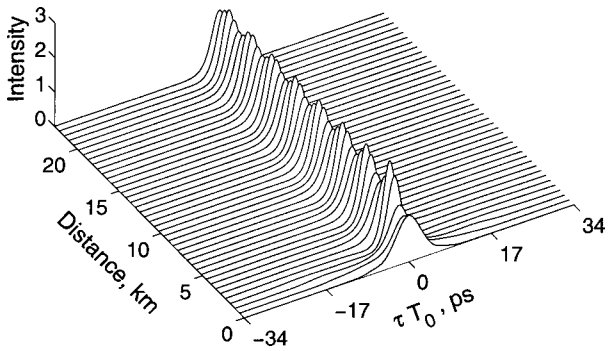

Fig. 5. Evolution of the transmitted pulse of Fig. 2(a) in a lossless fiber with constant dispersion identical to the initial dispersion $\beta_2(0)$ of the DDF loop.

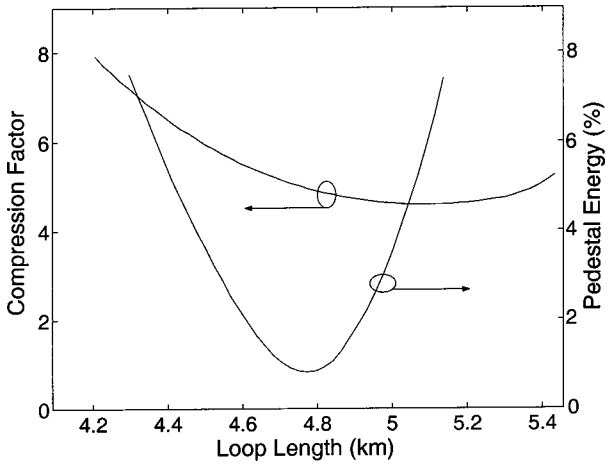

Fig. 6. Variation of the compression factor and corresponding pedestal energy with the loop length. In all cases, the input pulse is a sixth-order soliton with $T_{\text{FWHM}} = 30$ ps, and the dispersion decreasing rate of the loop is identical to that used in Fig. 2.

We next consider how the effective amplification (G_{eff}) of the DDF affects soliton generation. Figure 7 shows the compression factor, pedestal energy, and corresponding optimum loop length as a function of G_{eff} for a fixed input soliton with $N = 6$ and $T_{\text{FWHM}} = 30$ ps. For each value of G_{eff}, we optimized the compression by choosing an optimum loop length (i.e., an optimum dispersion-decreasing rate of the DDF). Figure 7 shows that both the compression factor and the pedestal energy increase with G_{eff}, while the optimum loop length z_{opt} is less affected by G_{eff}. For $G_{\text{eff}} > 3.6$, compression factors higher than 7.5 can be achieved, but the pedestal energy exceeds 10%. So, for soliton pulse generation, it is not possible to increase the compression factor by arbitrarily increasing G_{eff}. This is quite different from the adiabatic compression of a fundamental soliton in DDF, where the compression factor is equal to G_{eff}.

Figure 8 shows the effect of incident soliton order N on the compression factor, pedestal energy, and

optimum loop length. For all values of N studied here, the incident solitons have a same initial width of $T_{\mathrm{FWHM}} = 30$ ps, and the effective amplification of the loop is fixed at $G_{\mathrm{eff}} = 3$. Figure 8 shows that the compression factor increases with increasing soliton order N, while the optimum loop length decreases. The pedestal energy is very small for $N > 6$ but increases rapidly when N decreases from 6 to 4. Thus the compression is more suitable for incident solitons with larger soliton order. For example, for $N = 15$, a compression factor as high as 12 can be achieved with pedestal energy less than 0.2% with a loop length of 1.19 km.

C. Effect of Initial Frequency Chirp

The above studies assume that the incident pulses are transform limited. In practice, pulses generated from some lasers such as directly modulated semiconductor lasers are inherently chirped. In this subsection, we study the effect of initial frequency chirp on soliton compression in DD-NOLM.

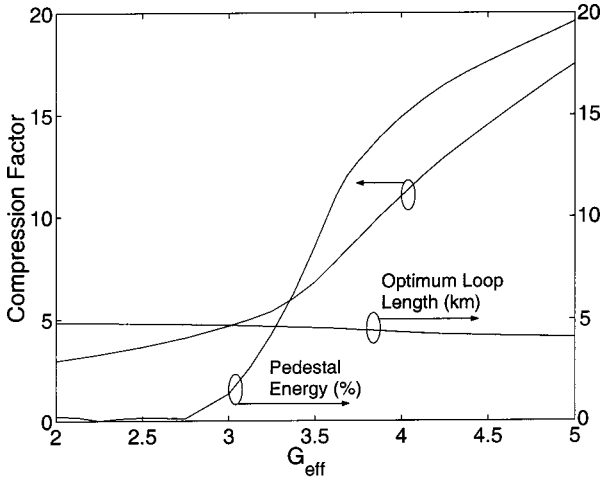

Fig. 7. Variation of the compression factor, pedestal energy, and corresponding optimum loop length with the effective amplification (G_{eff}). In all cases, the input soliton order is fixed at $N = 6$ with $T_{\mathrm{FWHM}} = 30$ ps.

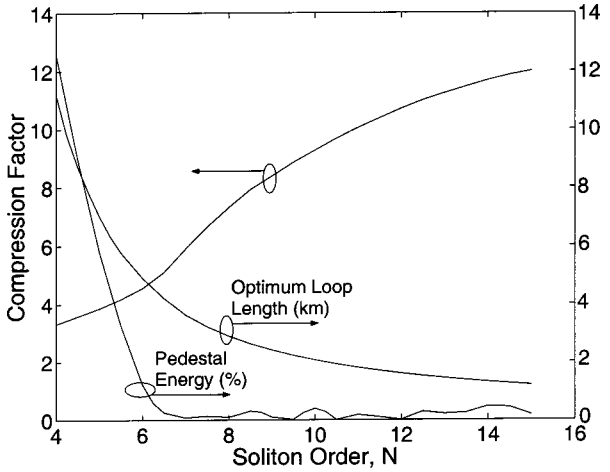

Fig. 8. Variation of the compression factor, pedestal energy, and optimum loop length with input soliton order N. For all values of N, the loop has an effective amplification of $G_{\mathrm{eff}} = 3$, and the input soliton width is fixed at $T_{\mathrm{FWHM}} = 30$ ps.

Table 1. Compression Results for Input Pulses with $N = 6$, $T_{\mathrm{FWHM}} = 30$ ps, $C = 2, -2$, and 4, and Effective Amplification of Loop Fixed at $G_{\mathrm{eff}} = 3$

Chirp parameter, C	2	−2	4
Compression factors	6.41	7.20	7.83
Pedestal energies (%)	0.23	15.67	0.79
Normalized intensities	2.72	1.07	4.04
Compressed soliton orders	1.55	0.86	1.54
Time–bandwidth products	0.38	0.39	0.37
Optimum loop lengths (km)	3.57	6.00	2.87

A linearly chirped incident pulse is given by [compare with Eq. (10)]

$$u_1(0, \tau) = N \operatorname{sech}(\tau) \exp(-iC\tau^2/2), \tag{15}$$

where C is the chirp parameter. Figures 9(a)–9(c) show the optimally compressed pulse shapes (solid curves) for $C = 2, -2$, and 4, respectively. In each case the incident pulse has the same intensity ($N = 6$) and the same initial width ($T_{\mathrm{FWHM}} = 30$ ps). The effective amplification of the DDF loop is fixed at $G_{\mathrm{eff}} = 3$, and the loop length is chosen to minimize the pedestal of the compressed pulse. The dashed curve in each case represents a hyperbolic-secant pulse having the same peak intensity and FWHM as those of the compressed pulse. Table 1 lists the compression results corresponding to Fig. 9. It shows that the technique is more tolerant of positive chirp than negative chirp. Compared with the zero chirp case (Fig. 2(a)), positive chirp increases the compression factor and the pulse quality and decreases the optimum loop length because anomalous GVD compresses positively chirped pulses linearly. Negative chirp, on the other hand, degrades pulse compression, contrary to conventional soliton-effect pulse compression.[35] We observed that although the compression factor for $C = -2$ is even larger than that for $C = 2$, the pulse quality declines, and the corresponding optimum loop length is much longer than that of the positive chirp. The reason is that the optimization criterion here is different from that of the soliton-effect compression technique, i.e., the fiber length is chosen to minimize the pulse pedestal rather than maximize the compression.

Figures 10(a)–10(c) show the evolution of the compressed pulses corresponding to Figs. 9(a)–9(c) in a constant-dispersion lossless fiber with dispersion coefficient identical to the initial dispersion coefficient $\beta_2(0)$ of the DDF loop. The evolution distance in each case is identical to that of Fig. 5 and is 22.7 km. We observed that the pulses evolve into fundamental solitons. In the case of $C > 0$, the evolved soliton has a narrower width than that of the initial pulse because the initial pulse has a soliton order $N > 1$. For $C < 0$, the initial soliton order is 0.86, so the width of the asymptotic soliton increases.

We then compare the chirp tolerance level of this technique to that of the adiabatic pulse compression. As mentioned before, adiabatic pulse compression is based on the robustness of fundamental solitons under weak perturbation such as dispersion. In the presence of initial frequency chirp, it had been shown[36] that a fundamental soliton can survive only for $|C|$ less than a critical

value of 1.64. In this regard, the soliton-generation scheme proposed here is more tolerant of initial frequency chirps than the adiabatic-compression technique. This is important for soliton generation from directly modulated semiconductor lasers since pulses produced by these lasers usually have strong frequency chirps.

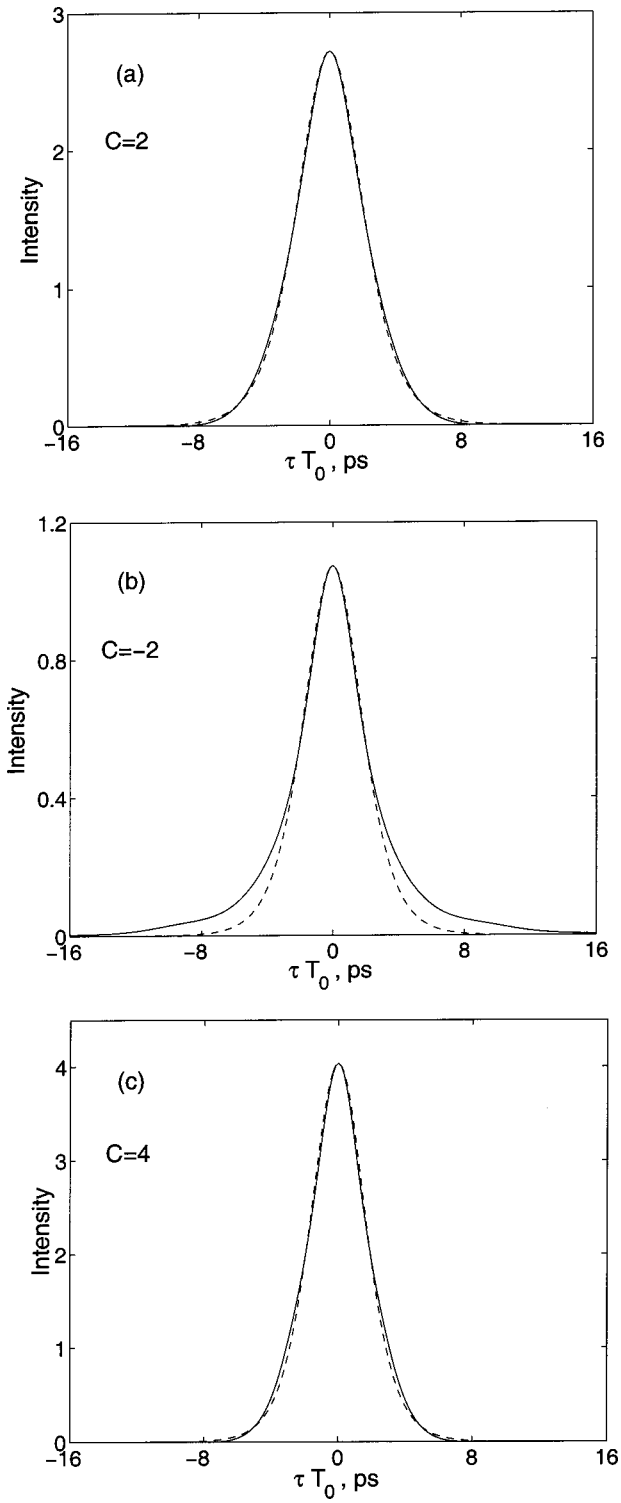

Fig. 9. Optimally compressed pulse shapes for $N = 6$, $T_{\mathrm{FWHM}} = 30$ ps, and with initial chirps of (a) $C = 2$, (b) $C = -2$, and (c) $C = 4$. In all cases the effective amplification of the loop is fixed at $G_{\mathrm{eff}} = 3$. The dashed curve in each case represents a hyperbolic-secant pulse having the same peak intensity and width (FWHM) as those of the compressed pulse.

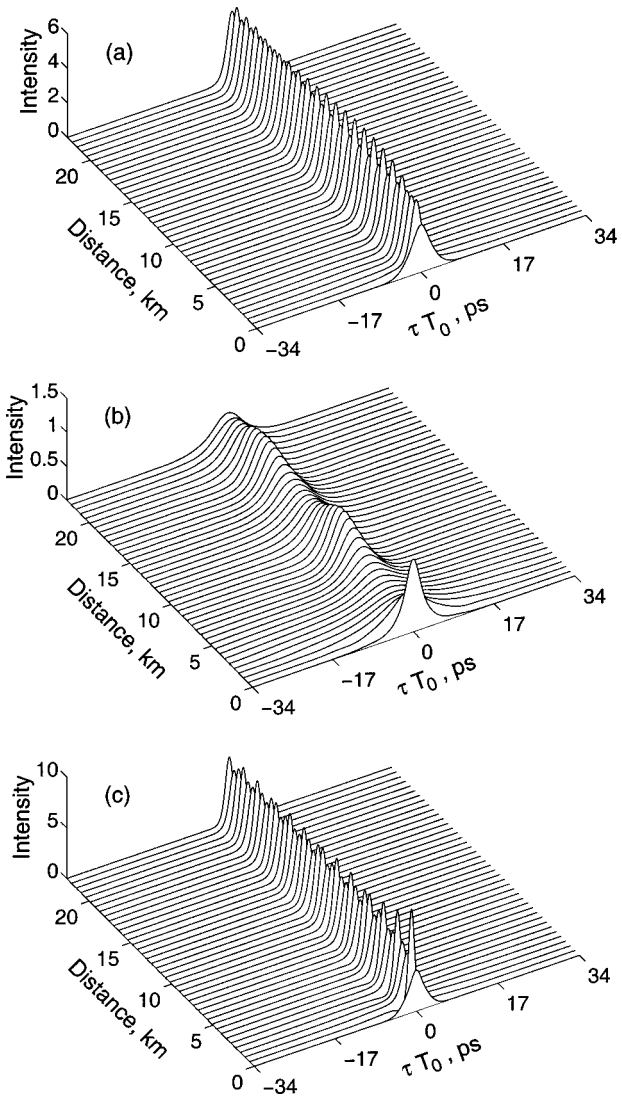

Fig. 10. Evolution of the compressed pulses corresponding to the solid curves of Figs. 9(a)–9(c) in a lossless fiber with constant dispersion identical to the initial dispersion $\beta_2(0)$ of the DDF loop.

We note that a linear frequency chirp can be precompensated by a linear dispersive element such as a grating pair, a prism pair, or a chirped fiber Bragg grating operating in reflection.[37] The use of these additional elements will increase system complexity, cause energy loss, and may deform the pulse shape. For example, the performance of a fiber Bragg grating is easily affected by TOD and RSS.[38] We have shown here that the DD-NOLM can produce high-quality compressed pulses even without precompensation of the initial frequency chirp.

D. Influence of Higher-Order Effects

The results presented so far concentrate on long pulse ($T_{\mathrm{FWHM}} > 5$ ps) compression in order to emphasize that the proposed scheme can overcome the difficulty of the adiabatic compression of input pulses longer than 5 ps in which impractically long lengths of fiber are required. For compression of ultrashort pulses ($T_{\mathrm{FWHM}} < 5$ ps), fi-

ber length is no longer a problem for the adiabatic technique. However, it was shown[10] that higher-order effects such as RSS and TOD become important since fibers used for adiabatic compression are usually several soliton periods long. Higher-order effects not only degrade the compression factor but also induce oscillations around the compressed pulse. In this final subsection, we investigate how higher-order effects affect soliton compression in a DD-NOLM.

Figure 11 shows the optimally compressed pulse shapes for the cases of (i) without RSS and TOD (dotted curve), (ii) with both RSS and TOD (solid curve), and (iii) with RSS only (dashed curve). In each case, the incident soliton was the same with $N = 6$ and $T_{\mathrm{FWHM}} = 1$ ps, and the effective amplification was fixed at $G_{\mathrm{eff}} = 3$. The self-steepening effect was neglected because it plays a much smaller role as compared with RSS or TOD. Assuming that $\beta_2(0) = -20\,\mathrm{ps}^2/\mathrm{km}$ and $\beta_3 = 0.1\,\mathrm{ps}^3/\mathrm{km}$, and that the Raman resonant time constant is $T_R = 3$ fs, according to Eq. (3), we have $\tau_R \approx 0.0053$, $\delta \approx 0.00147$, and $\Gamma \approx 0.00037$. Table 2 lists the compression results corresponding to Fig. 11. The results are somewhat surprising, since the compression seems to be quite forgiving to higher-order effects even when the compressed pulse is narrower than 100 fs. Unlike adiabatic soliton compression[10] in which TOD causes oscillations around compressed pulse, no oscillations appear in the present case because they are reflected by the DD-NOLM. The most interesting feature is that, under certain conditions, RSS can even improve the DD-NOLM performance. The compression factor is doubled, while the pedestal energy increases from 6.15% to 13.76% only. We note that, even if we allow pedestal energy comparable to 13.67% in the ideal case by choosing a shorter loop, the final compression factor is still smaller than that when only RSS is included.

The enhancement of soliton compression by RSS can be understood as follows. Since the loop dispersion is asymmetric, the counterpropagating pulses experience different RSS in the loop, resulting in a relative arrival time

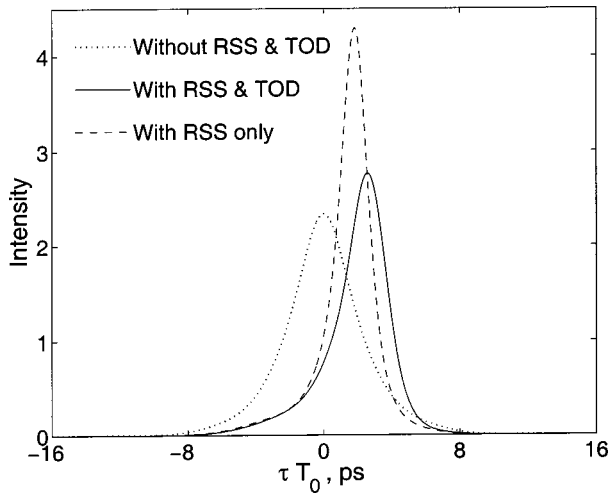

Fig. 11. Optimally compressed shapes of a 1-ps sixth-order soliton without RSS and TOD (dotted curve), with both RSS and TOD (solid curve), and with RSS only (dashed curve). In all cases, the effective amplification of the loop is $G_{\mathrm{eff}} = 3$.

Table 2. Compression Results of a 1-ps Sixth-Order Soliton without RSS and TOD, with both RSS and TOD, and with RSS only, where the Effective Amplification of the Loop is $G_{\mathrm{eff}} = 3$

Condition	Without RSS & TOD	With RSS & TOD	With RSS only
Compression factors	7.03	10.35	14.59
Pedestal energies (%)	6.15	10.18	13.67
Normalized intensities	2.33	2.75	4.24
Compressed soliton orders	1.30	0.96	0.85
Time–bandwidth products	0.35	0.37	0.37
Optimum loop lengths (m)	4.80	4.18	4.14

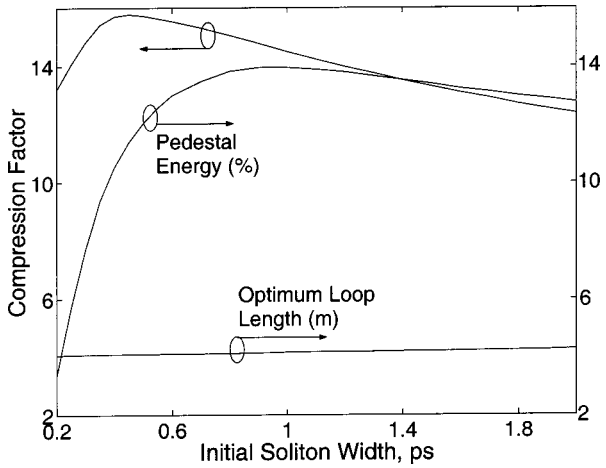

Fig. 12. Variation of the compression factor, pedestal energy, and optimum loop length with initial soliton width T_{FWHM} when only RSS is included. In each case the input is a sixth-order soliton, and the effective amplification of the loop is $G_{\mathrm{eff}} = 3$.

delay at the coupler. When the time delay increases, the overlap region of the two pulses is narrower than that when RSS is not included. Thus the region where the switching condition is satisfied decreases, leading to a shorter transmitted pulse. To study how the compression enhancement depends on RSS, we performed simulations for different initial soliton width T_{FWHM}. Figure 12 shows the compression factor, pedestal energy, and optimum loop length as a function of the initial soliton width T_{FWHM}. Only RSS is included, which is possible with a loop constructed from dispersion-flattened fiber to eliminate TOD. In all cases, the input is a sixth-order soliton and the effective amplification is fixed at $G_{\mathrm{eff}} = 3$. Figure 12 shows that RSS has little effect on optimum loop length but has a relatively large effect on the compression factor and pedestal energy. When T_{FWHM} increases, the enhancement in soliton compression declines because the compression approaches that of the ideal case, and the effect of RSS decreases. When the pulse width of the incident soliton is too short, compression enhancement also degrades because the temporal separation of the counterpropagating pulses is so large

that the two pulses almost separate before experiencing enough compression and before the switching condition is satisfied. So, for a given input soliton order and a fixed loop structure, there exists an optimum initial soliton width at which RSS induced compression enhancement is maximum.

4. CONCLUSIONS

We have proposed and demonstrated a technique to use a NOLM constructed from DDF to generate ultrashort fundamental solitons from long pulses. It uses both the multisoliton pulse-compression effect and the switching characteristics of a nonlinear optical loop mirror. The proposed scheme has the following advantages when compared with the conventional soliton-effect compression technique or the adiabatic-compression technique. First, long pulses (>30 ps) can be efficiently compressed with reasonable fiber lengths, and the compressed pulses are of high quality such that they evolve into fundamental solitons. Second, the proposed scheme is quite tolerant of initial frequency chirp, which is important for compression of pulses produced by directly modulated semiconductor lasers, since these pulses are inherently chirped. Third, for ultrashort pulse compression, higher-order effects such as RSS and TOD have a smaller effect on the new scheme. We also find that RSS can even enhance pulse compression significantly under certain conditions. A shortcoming of this technique is that, for a given input pulse, the compression factor is smaller than that of the conventional soliton-effect pulse compression because high pulse quality is achieved at the expense of the compression of the counterpropagating pulses in DD-NOLM. Nevertheless, the solitonlike pulses generated by this technique can be further compressed if they are coupled into a DDF, through which adiabatic soliton compression is possible, and the DDF length no longer presents a problem.

ACKNOWLEDGMENTS

The authors acknowledge the support of the Research Grant Council of the Hong Kong Special Administrative Region, China (project PolyU5096/98E), the National Natural Science Foundation of China (project 60277016), and the Guangdong Natural Science Foundation, China (project 021357).

*Permanent address, School of Information, Wuyi University, Guangdong 529020, China.

REFERENCES

1. G. P. Agrawal, *Fiber-Optic Communication Systems*, 2nd ed. (Wiley, New York, 1997).
2. M. Nakazawa, H. Kubota, K. Suzuki, E. Yamada, and A. Sahara, "Ultrahigh-speed long-distance TDM and WDM soliton transmission technologies," IEEE J. Sel. Top. Quantum Electron. **6**, 363–396 (2000).
3. L. F. Mollenauer, R. H. Stolen, and J. P. Gordon, "Experimental observation of picosecond pulse narrowing and solitons in optical fibers," Phys. Rev. Lett. **45**, 1095–1098 (1980).
4. K. A. Ahmed, K. C. Chan, and H. F. Liu, "Femtosecond pulse generation from semiconductor lasers using the soliton-effect compression technique," IEEE J. Sel. Top. Quantum Electron. **1**, 592–600 (1995).
5. K. C. Chan and H. F. Liu, "Short pulse generation by higher order soliton-effect compression: effects of optical fiber characteristics," IEEE J. Quantum Electron. **31**, 2226–2235 (1995).
6. S. V. Chernikov and P. V. Mamyshev, "Femtosecond soliton propagation in fibers with slowly decreasing dispersion," J. Opt. Soc. Am. B **8**, 1633–1641 (1991).
7. S. V. Chernikov, E. M. Dianov, D. J. Richardson, and D. N. Payne, "Soliton pulse compression in dispersion-decreasing fiber," Opt. Lett. **18**, 476–478 (1993).
8. M. D. Pelusi and H. F. Liu, "Higher order soliton pulse compression in dispersion-decreasing optical fibers," IEEE J. Quantum Electron. **33**, 1430–1439 (1997).
9. K. R. Tamura and M. Nakazawa, "Femtosecond soliton generation over a 32 nm wavelength range using a dispersion-flattened dispersion-decreasing fiber," IEEE Photon. Technol. Lett. **11**, 319–321 (1999).
10. K. T. Chan and W. H. Cao, "Enhanced compression of fundamental solitons in dispersion decreasing fibers due to the combined effects of negative third-order dispersion and Raman self-scattering," Opt. Commun. **184**, 463–474 (2000).
11. R. H. Stolen, J. Botineau, and A. Ashkin, "Intensity discrimination of optical pulses with birefringent fibers," Opt. Lett. **7**, 512–514 (1982).
12. B. Nikolaus, D. Grischkowsky, and A. C. Balant, "Optical pulse reshaping based on the nonlinear birefringence of single-mode optical fibers," Opt. Lett. **8**, 189–191 (1983).
13. R. Yatsu, K. Taira, and M. Tsuchiya, "High-quality sub-100-fs optical pulse generation by fiber-optic soliton compression of gain-switched distributed-feedback laser-diode pulses in conjunction with nonlinear optical fiber loops," Opt. Lett. **24**, 1172–1174 (1999).
14. K. R. Tamura and M. Nakazawa, "Spectral-smoothing and pedestal reduction of wavelength tunable quasi-adiabatically compressed femtosecond solitons using a dispersion-flattened dispersion-imbalanced loop mirror," IEEE Photon. Technol. Lett. **11**, 230–232 (1999).
15. M. D. Pelusi, Y. Matsui, and A. Suzuki, "Pedestal suppression from compressed femtosecond pulses using a nonlinear fiber loop mirror," IEEE J. Quantum Electron. **35**, 867–874 (1999).
16. K. R. Tamura and M. Nakazawa, "A polarization-maintaining pedestal-free femtosecond pulse compressor incorporating an ultrafast dispersion-imbalanced nonlinear optical loop mirror," IEEE Photon. Technol. Lett. **13**, 526–528 (2001).
17. K. Smith, N. J. Doran, and P. G. J. Wigley, "Pulse shaping, compression, and pedestal suppression employing a nonlinear-optical loop mirror," Opt. Lett. **15**, 1294–1296 (1990).
18. A. L. Steele, "Pulse compression by an optical fiber loop mirror constructed from two different fibers," Electron. Lett. **29**, 1972–1974 (1993).
19. I. Y. Khrushchev, I. H. White, and R. V. Penty, "High-quality laser diode pulse compression in dispersion-imbalanced loop mirror," Electron. Lett. **34**, 1009–1010 (1998).
20. L. Chusseau and E. Delevague, "250-fs optical pulse generation by simultaneously soliton compression and shaping in a nonlinear optical loop mirror including a weak attenuation," Opt. Lett. **19**, 734–736 (1994).
21. J. Wu, Y. Li, C. Lou, and Y. Gao, "Optimization of pulse compression with an unbalanced nonlinear optical loop mirror," Opt. Commun. **180**, 43–47 (2000).
22. S. V. Chernikov, J. R. Taylor, and R. Kashyap, "Experimental demonstration of step-like dispersion profiling in optical fiber for soliton pulse generation and compression," Electron. Lett. **30**, 433–435 (1994).
23. S. V. Chernikov, J. R. Taylor, and R. Kashyap, "Comblike dispersion-profiled fiber for soliton pulse train generation," Opt. Lett. **19**, 539–541 (1994).
24. P. V. Mamyshev, S. V. Chernikov, and E. M. Dianov, "Gen-

eration of fundamental soliton train for high-bit-rate optical fiber communication lines," IEEE J. Quantum Electron. **27**, 2347–2355 (1991).
25. S. V. Chernikov, D. J. Richardson, R. I. Laming, E. M. Dianov, and D. N. Payne, "70 Gbit/s fiber based source of fundamental solitons at 1550 nm," Electron. Lett. **28**, 1210–1212 (1992).
26. A. V. Shipulin, D. G. Fursa, E. A. Golovchenko, and E. M. Dianov, "High repetition rate cw fundamental soliton generation using multisoliton pulse compression in a varying dispersion fiber," Electron. Lett. **29**, 1401–1403 (1993).
27. A. V. Shipulin, E. M. Dianov, D. J. Richardson, and D. N. Payne, "40 GHz soliton train generation through multisoliton pulse propagation in a dispersion varying optical fiber circuit," IEEE Photon. Technol. Lett. **6**, 1380–1382 (1994).
28. A. L. Steele and J. P. Hemingway, "Nonlinear optical loop mirror constructed from dispersion decreasing fiber," Opt. Commun. **123**, 487–491 (1996).
29. J. L. S. Lima and A. S. B. Sombra, "Soliton and quasi-soliton switching in nonlinear optical loop mirror constructed from dispersion decreasing fiber," Opt. Commun. **163**, 292–300 (1999).
30. A. Boskovic, S. V. Chernikov, and J. R. Taylor, "Femtosecond figure of eight Yb:Er fiber laser incorporating a dispersion decreasing fiber," Electron. Lett. **31**, 1446–1448 (1995).
31. G. P. Agrawal, *Nonlinear Fiber Optics*, 2nd ed. (Academic, Boston, Mass., 1995), Chapts. 5 and 6.
32. A. Mostofi, H. Hatami-Hanza, and P. L. Chu, "Optimum dispersion profile for compression of fundamental solitons in dispersion decreasing fibers," IEEE J. Quantum Electron. **33**, 620–628 (1997).
33. A. Hasegawa, *Optical Solitons in Fibers* (Springer-Verlag, Berlin, 1989).
34. N. J. Doran and D. Wood, "Nonlinear-optical loop mirror," Opt. Lett. **13**, 56–58 (1988).
35. K. C. Chan and H. F. Liu, "Effects of Raman scattering and frequency chirping on soliton-effect pulse compression," Opt. Lett. **18**, 1150–1152 (1993).
36. C. Desem and P. L. Chu, "Effect of chirping on soliton propagation in single-mode optical fibers," Opt. Lett. **11**, 248–250 (1986).
37. J. D. Minelly, A. Galvanauskas, M. E. Fermann, D. Harter, J. E. Caplen, Z. J. Chen, and D. N. Payne, "Femtosecond pulse amplification in cladding-pumped fibers," Opt. Lett. **20**, 1797–1799 (1995).
38. G. P. Agrawal, *Applications of Nonlinear Fiber Optics* (Academic, Boston, Mass., 2001), Chapt. 6.